IEEE Photonics Journal
An IEEE Photonics Society Publication

Open Access

Characterize the Speed of a Photon-Number-Resolving Superconducting Nanowire Detector

Volume 12, Number 4, August 2020

Xu Tao
Hao Hao
Xiang Li
Shi Chen
Libo Wang
Xuecou Tu
Xiaoqing Jia
Labao Zhang
Qingyuan Zhao
Lin Kang
Peiheng Wu

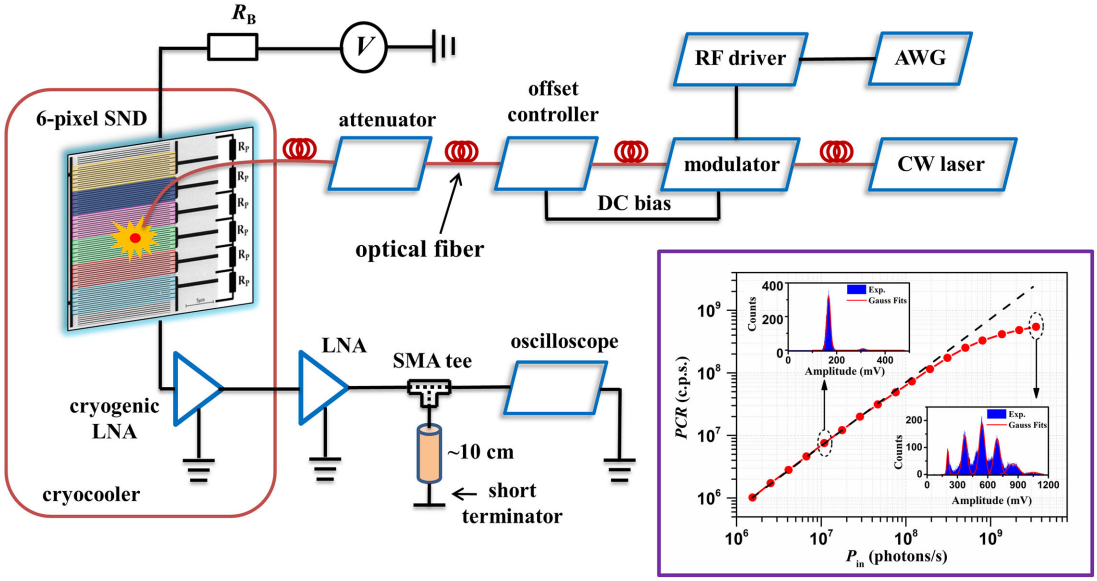

DOI: 10.1109/JPHOT.2020.3012349

Characterize the Speed of a Photon-Number-Resolving Superconducting Nanowire Detector

Xu Tao,[1] **Hao Hao**,[1] **Xiang Li**,[1] **Shi Chen**,[1] **Libo Wang**,[1] **Xuecou Tu**,[1,2] **Xiaoqing Jia**,[1,2] **Labao Zhang**,[1,2] **Qingyuan Zhao**,[1,2] **Lin Kang**,[1,2] **and Peiheng Wu**[1,2]

[1]Research Institute of Superconductor Electronics (RISE), School of Electronic Science and Engineering, Nanjing University, Nanjing, Jiangsu 210023, China
[2]Purple Mountain Laboratories, Nanjing, Jiangsu 211111, China

DOI:10.1109/JPHOT.2020.3012349

Manuscript received June 19, 2020; revised July 18, 2020; accepted July 22, 2020. Date of publication July 28, 2020; date of current version August 12, 2020. This work was supported in part by the National Key R&D Program of China under Grant 2017YFA0304002, in part by the National Natural Science Foundation under Grants 61521001, 61801206, 61571217, 61801209, and 11227904, in part by the Recruitment Program for Young Professionals, in part by the Program for Innovative Talents and Entrepreneur in Jiangsu, in part by the Fundamental Research Funds for the Central Universities, in part by the Priority Academic Program Development of Jiangsu Higher Education Institutions (PAPD), in part by the Qing Lan Project, and in part by the Jiangsu Provincial Key Laboratory of Advanced Manipulating Technique of Electromagnetic Waves. (The authors contributed equally to this work.)
Corresponding authors: Qingyuan Zhao; Lin Kang (e-mail: qyzhao@nju.edu.cn; kanglin@nju.edu.cn)

Abstract: Superconducting series nanowire single-photon detectors (SNDs) have been used for resolving photon numbers. But it can also exhibit a higher counting rate than a single superconducting nanowire single-photon detector (SNSPD), because the serial architecture allows multiple detectors working in parallel and the inductance of each pixel is reduced. In this paper, we found each pixel of the SND could reset fast although the whole detector took a much longer time for recovering. Therefore, the speed of an SND with a large kinetic inductance of 1.25 μH was characterized and compared to a standard SNSPD with the same total inductance. By measuring the detected photon rate over the input photon rate, we obtained a photon counting rate enhancement by 7.5 times. Meanwhile, the timing jitter of the SND was 63 ps at single photon detection regime. Our results show that the series structure and the readout scheme are quite practical in realizing high speed single-photon detectors besides resolving photon numbers.

Index Terms: High-speed photon counting, superconducting single-photon detector, series nanowire.

1. Introduction

High-speed superconducting nanowire single-photon detectors (SNSPDs) are of interest for a range of single photon counting applications such as laser radar [1], optical communications [2] and single-photon imaging [3]. For fiber coupled applications, SNSPDs are designed with a large active area for matching the fiber diameter, which has a limited counting rate of a few tens of MHz due to a large kinetic inductance of the superconducting nanowires [4]. The coupling capacitor between the detector and the RF amplifier in the readout causes an overshoot of the bias current at high counting rates, giving a limit for the maximum counting rate that can be reached reliably

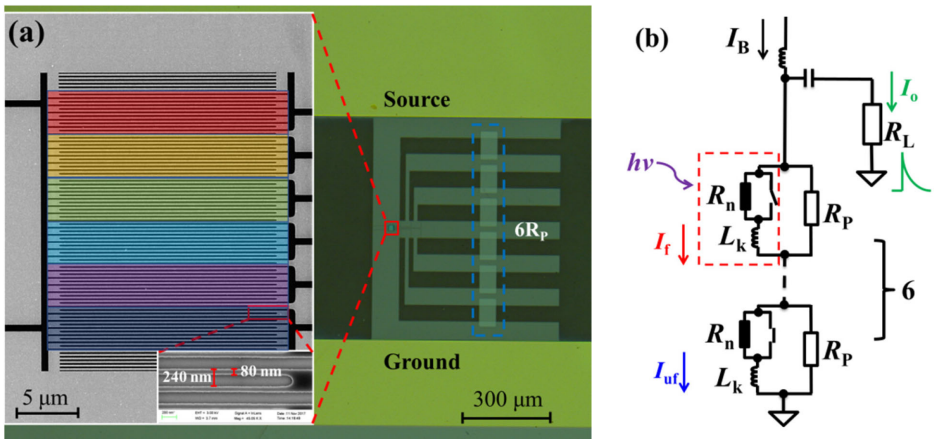

Fig. 1. (a) Device structure of the 6-pixel NbN SND. (b) Equivalent circuit model of the 6-pixel SND.

[5]. SNSPD arrays can provide a high counting rate by operating multiple detectors in parallel [6,] [7], [8], however, they require more connections or multiplexing readout circuits [9], [10]. The series nanowire superconducting single-photon detector (SND), which is originally aimed for photon-number-resolving (PNR) applications [11], [12], is a relatively simple array architecture that uses only on-chip resistors for synthesizing the output signals from fired nanowires into one output for external access [13]. The readout circuit of an SND is the same as that of a standard SNSPD, greatly reducing the readout complexity.

Recently, we fabricated a large area ($\sim$20 $\times$ 20 μm^2) SND with a total kinetic inductance of 1.25 μH, which had a pulse recovery time of $\sim$50 ns, but the PNR detector demonstrated a potential of high counting rate [14]. In this work, we found that the increase of counting rates was attributed to the series array architecture and the weak dependence of detection efficiency on bias current. Each nanowire of the SND detector can reset fast, although the whole device took a much longer time for recovering. Therefore, it cannot directly estimate the counting rate performance from the output pulses like conventional SNSPDs. To better understand and characterize the speed of an SND, we created a circuit model to find the current recovery of each nanowire and measured the photon counting rate of a 6-pixel SND over the input photon rate for extracting the dependence of counting rates on the detection efficiency. The 6-pixel SND realized a photon rate of 380 MHz, enhanced by 7.5 times in comparison to a standard SNSPD with the same inductance. Otherwise, a timing jitter of 63 ps at single photon detection regime was obtained. Our results proved that the proposed structure and the readout scheme are quite practical in realizing high speed single-photon detectors. And the SND also provided a solution to the major drawback for direct fiber-coupled and free-space-coupled SNSPDs that a large active area slows the detector down due to an increase of the kinetic inductance of the nanowires.

2. Device Simulation

As Fig. 1(a) shows, the detector characterized in our measurements is a NbN SND with 6 series pixels. Each pixel is a short meander nanowire shunted by a resistor R_{P}. It was fabricated by a 5 nm thick NbN film, which had a sheet resistance of $R_{\square} = 300\ \Omega/\square$ at room temperature and a critical temperature of $T_{\mathrm{C}} = 7$ K. The active area of the device was $\sim$20 $\times$ 20 μm^2, the width of the nanowire was 80 nm wide with a pitch of 240 nm, and the total nanowire length of each pixel was 213 μm. An optical cavity was manufactured on the substrate and the detector was fiber coupled with a single-mode fiber on the backside. The beam spot was focused to the active area with a focusing dual-lens, which had a coupling efficiency of more than 95% [15]. At 2.1 K, the detector

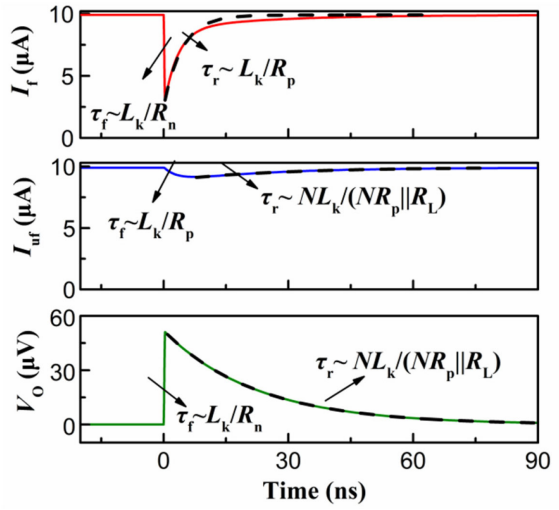

Fig. 2. The simulation results of the 6-pixel SND taking into account device parameters. A photon detection event happens at 0 ns at one of the pixels. The top figure shows the current reduction and recovery through the fired nanowire, while the middle figure shows the current through the unfired nanowires. The bottom figure shows the output voltage on a 50 Ω load. The calculated time constants for each pulse are marked. The dashed lines are exponentially decayed curves with the approximate time constants marked nearby.

showed a critical current of $I_C = 10$ μA, a saturated system detection efficiency (SDE) of 68% at 1550 nm and a low DCR of 1 Hz, as the inset of Fig. 4(b) shows.

The equivalent circuit model of the SND was shown in Fig. 1(b). Each nanowire can be electrically equivalent to a switch-controlled resistor R_n in series with a kinetic inductor L_k. The wires had a sheet kinetic inductance of $L_\square = 78$ pH/□, giving a kinetic inductance of 208 nH for each pixel and 1.25 μH for the entire 6-SND. To avoid any latching or unwanted oscillation [16], each parallel resistance of R_P was designed to be 50 Ω. The bias current I_B was 9.9 μA and the readout load R_L was 50 Ω.

Here we use a nanowire SPICE model to simulate the nanowire transient response [17]. As shown in Fig. 1(b), when one of the nanowires detects a photon, the switch turns off and the transient resistor R_n goes from zero into the kΩ range within tens of ps. In the fired pixel, the current originally passing through the superconducting nanowire is then expelled primarily to R_P and R_L with a time constant of $\sim L_k/R_n$ since R_n is much larger than R_L and R_P. Thus, we see a sharp rising edge for the output voltage pulse V_O and a rapid reduction of current through the fired nanowire I_f, as shown in Fig. 2. Because the other pixels are not fired, the impedance of each unfired pixel is R_p // $j\omega L_k$, where ω is the angular frequency of the interested signals. For fast current dynamics, $j\omega L_k$ is much larger than R_p. Thus, the current through the unfired nanowire I_{uf} is almost unchanged. The output current on the load is approximate $I_O = (I_B - I_r)/(N + R_L/R_P)$, where I_r is the minimum current remained in the fired nanowire. The output voltage V_O is $I_O \cdot R_L$. For the recovery of currents, the fired nanowire returns to superconducting state and $R_n = 0$. Ignoring the slight change of currents through the unfired nanowires, the output voltage decays exponentially with a time constant of $\sim NL_k/(NR_p||R_L)$ while the current through the fired nanowire recovers exponentially with a time constant of $\sim L_k/R_p$, which is approximately N times faster. It indicates each wire of the series nanowire detector can reset fast, although the whole device takes a much longer time for recovering.

During the full photon detection event, the current through the unfired nanowire I_{uf} only has a slight reduction due to the current distribution to R_L. I_{uf} first reduces exponentially with a constant of $\sim L_k/R_p$, which is a much slower process than I_f. Then, it recovers exponentially with a time constant of $\sim NL_k/(NR_p||R_L)$. From our simulation results, I_{uf} reduces by ~0.7 μA, which is 7%

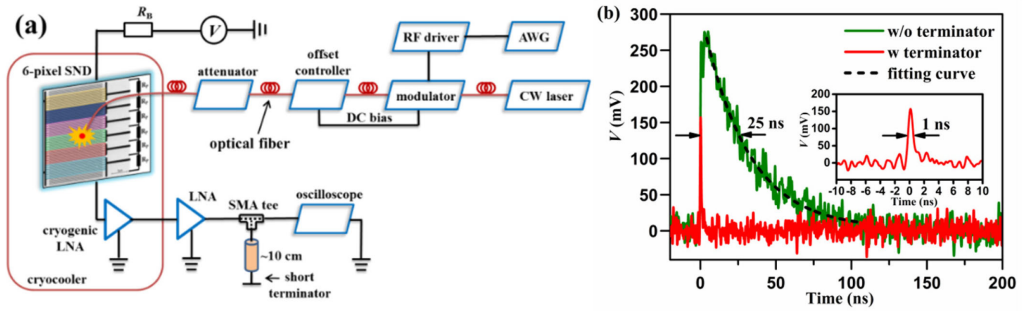

Fig. 3. (a) Schematic of the experimental setup to measure the speed of the SND. (b) A comparison of the pulses sampled from the readouts without/with the short terminator setup. The original pulse (green) has a pulse width of 25 ns, the dashed line of which is the exponentially decayed fitting curve. After the pulse shaping circuit, the pulse (red) preserves the fast leading edge for detecting and the width of the pulse presented in the inset is narrowed to only 1 ns, although the terminator also brings in some attenuations on the pulse amplitude.

of the critical current. Such a reduction of I_{uf} can be further decreased if a high input impedance amplifier is used to increase R_{L} [18]. It indicates that, although there is a long decay time for the output voltage pulse, the unfired nanowires are maintained at high bias levels ready for detecting the following photons. Therefore, the multiple pixels in an SND can operate in a parallel fashion, enabling high counting performance. However, photon detection events lead to current reduction through all the nanowires, which also decreases the efficiency of the detector especially at high counting rate. Therefore, an SND with saturated system detection efficiency is required to sustain a high efficiency when the current gets reduced because the efficiency could reach saturation at a relatively low current and is weakly dependent of the current at high bias.

It is worth noticing that our simulation of the recovery time only considered single-photon detection cases, because the detector can approach to its real speed only in the single photon regime. As more pixels are fired simultaneously, the recovery time of the fired pixels becomes longer. In the worst case that all six pixels fire together, the recovery time of the fired nanowires is the same as that of the output voltage. The current on the unfired nanowires I_{uf} is also further reduced, because a larger leakage current is distributed to R_{L}. The results are in agreement with what was discussed in Ref. [18] and indicate that multi-photon detection cases show negative effects on the photon counting rates.

3. Measurements and Discussion

To characterize the high-speed performance of the SND, we built a measurement setup shown in Fig. 3(a) to obtain the photon count rate (PCR). The SND was cooled at a temperature of 1.5 K and it was fiber-coupled to incident optical pulses. We used a high extinction ratio intensity electro-optic modulator and a continuous laser at 1550 nm wavelength to generate periodic optical pulses at a repetition rate of 1 GHz. The pulse width was regulated to be 125 ps by a fast arbitrary waveforms generator. The output detection pulses were first amplified by a commercial cryogenic amplifier (Caltech CITLF1) with a gain of 40 dB and then went to a room-temperature low-noise amplifier (LNA) with a gain of 32 dB. As we discussed above, the six nanowire detectors can operate parallelly. However, because of the relatively long reset time of the output pulse, multiple detections from separate pixels overlapped, giving a difficulty in distinguishing them. Therefore, a short-terminated coaxial cable ($\sim$10 cm) was connected at the output port of the LNA to cancel out the long falling edge while preserving the fast leading edge by inducing an inverted pulse with identical amplitude and a time delay of approximately 1 ns [19]. After the pulse shaping circuit, the pulse width (defined as the full width at half maximum value) was reduced from 25 ns to 1 ns,

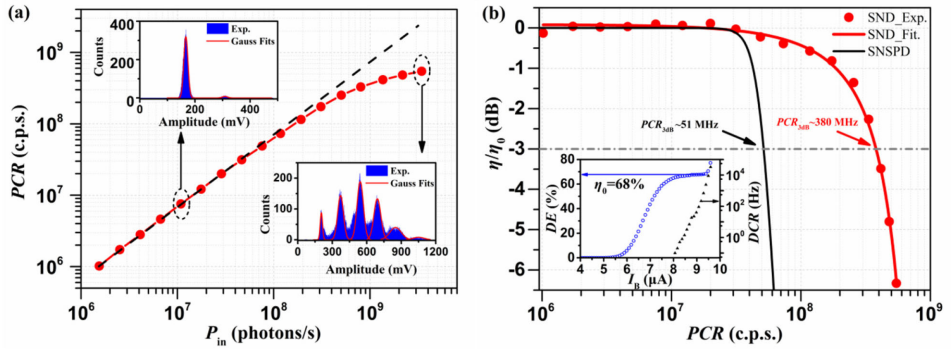

Fig. 4. (a) The detected *PCR* as a function of the input photon flux $P_{\rm in}$. The inserted figures show histograms of pulse counting rate over the pulse amplitude at a low photon flux and a high photon flux. The red lines are Gaussian fits to the histograms. (b) The normalized detection efficiency η/η_0 as a function of *PCR*. The red lines are the experimental and fitting results of the SND and the black line is the calculation result of a standard SNSPD with the same inductance in comparison. The inset shows the *SDE* and *DCR* of the SND as a function of $I_{\rm B}$. The saturation efficiency η_0 is 68% at $I_{\rm B} = 9.2\ \mu$A.

as Fig. 3(b) shows. Because the *PCR* measured was hundreds of MHz and there existed multiple photon events, we used a fast oscilloscope to acquire the output pulses and extracted the *PCR* after post-processing.

Fig. 4 shows our experimental results. First, we measured the dependence of the detected photon counting-rate on the input photon rates $P_{\rm in}$. The repetition rate of the incident light was fixed at 1 GHz and the SND was biased at 10 μA. By attenuating the input light power, we can set different $P_{\rm in}$. When $P_{\rm in}$ was high, the probability of multiple photon events went high in one optical pulse. For conventional SNSPD of no photon-number-resolving capability, *PCR* was equal to the rate of output voltage pulses. However, since SND was capable of resolving multiple photons at one output pulse, the photon rate was $PCR = \Sigma n \times CR_{\rm n}$, where n was the detected photon number and $CR_{\rm n}$ was the counting rate for detecting n photons. Fig. 4(a) illustrates the *PCR* vs. $P_{\rm in}$. At low photon flux, the *PCR* increased linearly with a slope of $\eta = PCR/P_{\rm in} = \eta_0$, where $\eta_0 = 68\%$ is the maximum SDE at single-photon detection regime. For example, we can see in the inset that the distribution of the pulse height at low photon flux (e.g. 1.1×10^7 photons/s) shows a single single-photon detection peak with a small two-photon detection peak. As the optical power increased for having more input photons, *PCR* grew up nonlinearly, indicating a reduction of the detection efficiency. Meanwhile, multi-photon detections were observed prominently. For example, there were six peaks of the pulse amplitude distribution at a high photon flux of 3.4×10^9 photons/s, corresponding to detecting 1$\sim$6 photons in one pulse.

Here we extract the dependence of photon counting rates on the detection efficiency. Fig. 4(b) plots the normalized system detection efficiency η/η_0 as a function of the *PCR*, where the red lines are the experimental and fitting results of the SND. The *PCR* is 104 MHz when the *SDE* has a 10% drop, the *PCR* is 380 MHz when the *SDE* drops 50% (-3 dB) and the *PCR* is 535 MHz when the *SDE* drops 75% (-6 dB). We compare the *PCR* of the SND to that of a standard SNSPD with the same total inductance. For a standard SNSPD with the same total inductance $L_{\rm t} = 6L_{\rm k} = 1.25\ \mu$H, the bias current would recover exponentially with a time constant of $L_{\rm t}/R_{\rm L} = 25$ ns. Supposing that the SNSPD has the same dependence of *SDE* on bias current, as shown in the inset of Fig. 4(b), we can get the dependence of *SDE* recovery on time, and thus plot the dependence of *SDE* on *PCR*, as the black line in Fig. 4(b) shows. For example, when the *SDE* is 50% of its peak value, the current is 6.7 μA ($0.67I_{\rm C}$). Therefore, we can calculate that it takes 19.6 ns for the standard SNSPD to recover to 50% of its peak value and the corresponding *PCR* is 51 MHz. Compared to the standard SNSPD with the same inductance, there is a speed enhancement by a factor of 7.5 for the SND when the *SDE* is at the 50% of its peak value.

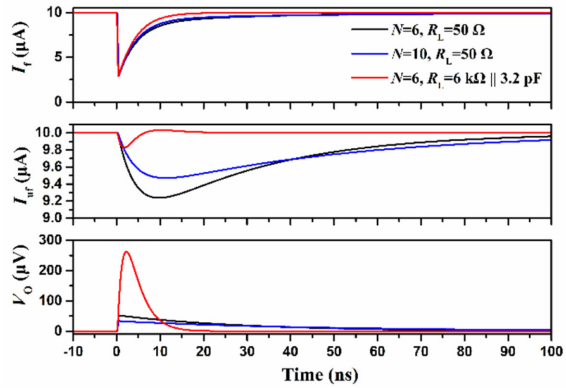

Fig. 5. Simulation results of the transient responses of a 10-pixel SND at $R_{\mathrm{L}} = 50\ \Omega$ and a 6-pixel SND at the input impedance of 6 kΩ in parallel with a capacitor of 3.2 pF in comparison to a 6-pixel SND at $R_{\mathrm{L}} = 50\ \Omega$, corresponding to the blue, red and black lines.

However, an ideal *N*-SNSPD array with identical total inductance is supposed to have an enhancement factor of N^2 (which was 36 for $N = 6$), since *N* SNSPDs work in parallel and the kinetic inductance of each SNSPD is reduced to 1/*N*. Compared to that, the speed enhancement of an SND we measured was underestimated, mainly because the maximum enhancement happened only when the incident photons were at a pure single-photon regime where only one photon was detected by one of the unfired pixels in one optical pulse. This condition was hardly achieved by using a classical optical source in our experiment. For high P_{in}, when multiple photons fired multiple pixels in one optical pulse, the number of unfired pixels being ready for detecting the following photons was reduced and the current through these unfired pixels was also reduced, which lowered the efficiency. Therefore, *SDE* decreased rapidly at high P_{in}.

The reasons for an underestimated speed of the SND also suggest approaches for further increasing the speed. Firstly, the recovery dynamics of an SND depend on the number of pixels as well. The blue lines in Fig. 5 are the simulation results of the transient response of a 10-pixel SND at $R_{\mathrm{L}} = 50\ \Omega$, which show a faster current reset of the fired nanowire and a reduced leakage current into R_{L} than that of a 6-pixel SND (black lines in Fig. 5) when a photon detection event happens. However, the pulse amplitude V_{O} is also reduced due to a reduced leakage current into R_{L}. Therefore, one approach is to develop an SND of more pixels so that multi-photon detections can also only deactivate a small portion of all pixels. But it is noting that the speed is improved at the sacrifice of the signal amplitude when increasing the number of pixels. *Mattioli et al.* demonstrated an SND with the pixel number of up to 24, which had a relatively low efficiency value but showed its application as a linear detector of analog signals at frequencies up to few hundred MHz [20]. Secondly, applying a high impedance readout supports fully estimating the speed of the SND and improving the signal to noise ratio. Due to a large R_{L}, the leakage current to R_{L} can be neglected. The current of the fired nanowires is entirely distributed to R_{P} and current through the unfired wires remains unvaried ($I_{\mathrm{uf}} = I_{\mathrm{B}}$). Therefore, the voltage on the unfired pixels is zero, and the output voltage is entirely produced by the fired pixels ($\sim(I_{\mathrm{B}} - I_{\mathrm{r}})\cdot R_{\mathrm{P}}$), which has an amplitude improvement by $(N + 1)$ times. Due to $R_{\mathrm{L}} >> NR_{\mathrm{P}}$, the output voltage recovers exponentially with a time constant of $NL_{\mathrm{k}}/(NR_{\mathrm{p}}||R_{\mathrm{L}}) \approx L_{\mathrm{k}}/R_{\mathrm{p}}$, which is equal to the current reset time of the fired nanowires. The dependence of the recovery time on the number of fired pixels is also minimized. Therefore, the pixels of the SND work independently from each other and the SND performs similar to an ideal *N*-SNSPD array if a high impedance readout is used. However, due to the coupling capacitor of the amplifier, it is challenging to realize an ultrahigh input impedance at high frequencies. We have designed a cryogenic RF amplifier with a low power dissipation of 0.9 mW and an equivalent input impedance of 6 kΩ || 3.2 pF at 4.2 K for the series nanowire detector [21], and more works on the interconnections and readout results will be covered in the future. The transient results of the

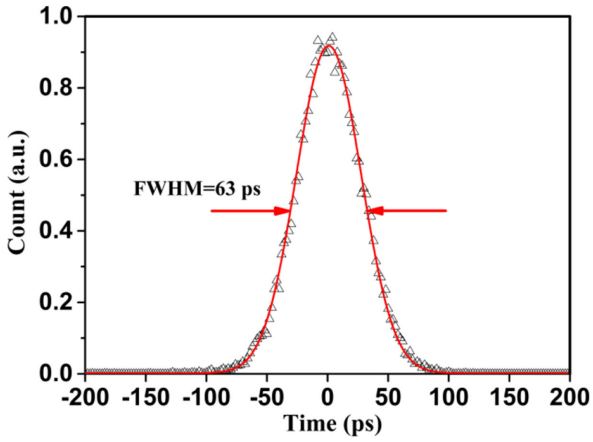

Fig. 6. Histogram of the normalized counts over delay time between the detected pulse and the reference of a fs laser. The bias current is set to 10 μA. The red solid line is the Gaussian fit. $T_{\rm j}$ is 63 ps defined as the FWHM value of the histogram.

6-pixel SND by the cryogenic RF amplifier with a capacitive input impedance of 6 kΩ || 3.2 pF are simulated by the red lines of Fig. 5, which show the advantage of a high impedance circuit on reading the series nanowire detector. Compared to that of the 6-pixel SND at $R_{\rm L} = 50\ \Omega$, $I_{\rm f}$ resets a litter faster with a time constant of 4.18 ns, and $I_{\rm uf}$ is weakly changed (decreased by 1.8%$I_{\rm C}$). The voltage amplitude is increased from 52 μV to 262 μV, and the voltage reset time, which is fitted to $\tau_{\rm r} \sim 4.37$ ns, is shorted approximately equal to the reset tine of $I_{\rm f}$.

Besides the fast counting rate, low timing jitter is another requirement for high-speed applications. The SND has a low timing jitter (T_j) as well. To measure the jitter, we changed the light source to a sub-ps pulsed laser at a wavelength of 1550 nm. The delay time between a detection pulse and the reference of the optical pulses was measured to create a histogram shown in Fig. 6. The photon flux was set to 2×10^6 photos/s to ensure the SND operating at single-photon detection regime. The measured timing jitter defined as the full width at half maximum (FWHM) of the histogram was 63 ps. It mainly originated from amplifier noise and mechanisms intrinsic to the detector. We estimated the jitter from the amplifier noise, which was 43 ps (the slope of the edge at the discrimination level was 0.565 mV/ps and the FWHM of the noise was 24.3 mV). Therefore, the intrinsic jitter of the 6-pixel detector was approximately 46 ps.

4. Conclusion

In summary, the series nanowire detector has demonstrated a single superconducting single-photon detector with a high photon counting rate of a few hundred MHz for fiber-coupled applications. The 6-pixel SND shows a photon-counting enhancement by a factor of 7.5 compared to a standard SNSPD with the same inductance, benefiting from its series architecture and weak dependence of the detection efficiency on bias current. Low timing jitter of 63 ps is obtained as well. These results suggest that the SND is not only promising for resolving photon numbers but also practical for high-speed photon counting applications.

References

[1] F. Scholder, J. D. Gautier, M. Wegmller, and N. Gisin, "Long-distance OTDR using photon counting and large detection gates at telecom wavelength," *Opt. Comm.*, vol. 213, no. 1, pp. 57–61, Nov. 2002.
[2] M. E. Grein *et al.*, "An optical receiver for the Lunar Laser Communication Demonstration based on photon-counting superconducting nanowires," in *Proc. SPIE*, vol. 9492, May, 2015.

[3] H. Zhou *et al.*, "Few-photon imaging at 1550 nm using a low-timing-jitter superconducting nanowire single-photon detector," *Opt. Express*, vol. 23, no. 11, pp. 14603–14611, 2015.
[4] A. J. Kerman *et al.*, "Kinetic-inductance-limited reset time of superconducting nanowire photon counters," *Appl. Phys. Lett.*, vol. 88, no. 11, Jan. 2006, Art. no. 111116.
[5] A. J. Kerman, D. Rosenberg, R. J. Molnar, and E. A. Dauler, "Readout of superconducting nanowire single-photon detectors at high count rates," *J. Appl. Phys.*, vol. 113, Mar. 2013, Art. no. 144511.
[6] D. Rosenberg, A. J. Kerman, R. J. Molnar, and E. A. Dauler, "High-speed and high-efficiency superconducting nanowire single photon detector array," *Opt. Express*, vol. 21, no. 2, pp. 1440–1447, 2013.
[7] J. Huang *et al.*, "High speed superconducting nanowire single photon detector with nine interleaved nanowires," *Supercond. Sci. Technol.*, vol. 31, no. 7, May 2018.
[8] W. J. Zhang *et al.*, "A 16-pixel interleaved superconducting nanowire single-photon detector array with a maximum count rate exceeding 1.5 GHz," *IEEE Trans. Appl. Supercond.*, vol. 25, no. 5, Aug. 2019, Art. no. 2200204.
[9] K. Makise, H. Terai, S. Miki, T. Yamashita, and Z. Wang, "Design and fabrication of all-NbN SFQ circuits for SSPD signal processing," *IEEE Trans. Appl. Supercond.*, vol. 23, no. 3, Jun. 2013, Art. no. 1100804.
[10] M. S. Allman *et al.*, "A near-infrared 64-pixel superconducting nanowire single photon detector array with integrated multiplexed readout," *Appl. Phys. Lett.*, vol. 106, no. 19, May 2015, Art. no. 192601.
[11] D. Sahin *et al.*, "Waveguide photon-number-resolving detectors for quantum photonic integrated circuits," *Appl. Phys. Lett.*, vol. 103, Aug. 2013, Art. no. 111116.
[12] E. Schmidt *et al.*, "Characterization of a photon-number resolving SNSPD using Poissonian and sub-Poissonian light," *IEEE Trans. Appl. Supercond.*, vol. 29, 2019, Art. no. 2201305.
[13] S. Jahanmirinejad *et al.*, "Photon-number resolving detector based on a series array of superconducting nanowires," *Appl. Phys. Lett.*, vol. 101, no. 135, Jul. 2012, Art. no. 072602.
[14] X. Tao *et al.*, "A high speed and high efficiency superconducting photon number resolving detector," *Supercond. Sci. Technol.*, vol. 32, no. 6, 2019, Art. no. 064002.
[15] L. B. Zhang *et al.*, "Dual-lens beam compression for optical coupling in superconducting nanowire single-photon detectors, " *Sci. Bull.*, vol. 60, no. 16, pp. 1434–1438, 2015.
[16] A. J. Kerman, J. K. W. Yang, R. J. Molnar, E. A. Dauler, and K. K. Berggren, "Electrothermal feedback in superconducting nanowire single-photon detectors," *Phys. Rev. B*, vol. 79, no. 10, pp. 101–104, 2009.
[17] K. K. Berggren *et al.*, "A superconducting nanowire can be modeled by using SPICE," *Supercond. Sci. Technol.*, vol. 31, no. 5, 2018, Art. no. 055010.
[18] S. Jahanmirinejad, and A. Fiore, "Proposal for a superconducting photon number resolving detector with large dynamic range," *Opt. Express*, vol. 20, no. 5, pp. 5017–5028, 2012.
[19] Q. Y. Zhao *et al.*, "Counting rate enhancements in superconducting nanowire single-photon detectors with improved readout circuits," *Opt. Lett.*, vol. 39, no. 7, pp. 1869–1872, 2014.
[20] F. Mattioli, Z. Zhou, A. Gaggero, R. Gaudio, R. Leoni, and A. Fiore, "Photon-counting and analog operation of a 24-pixel photon number resolving detector based on superconducting nanowires, " *Opt. Express*, vol. 24, no. 8, pp. 9067–9076, 2016.
[21] C. Wan, Z. Jiang, L. Kang, and P. H. Wu, "High input impedance cryogenic RF amplifier for series nanowire detector," *IEEE Trans. Appl. Supercond.*, vol. 27, no. 4, 2017, Art. no. 1502605.